

Mixing Characteristics of Urethane Based Materials and Polyurea in RIM

M. NELSON and L. JAMES LEE,* *Engineering Research Center for Net Shape Manufacturing and Department of Chemical Engineering, The Ohio State University, Columbus, Ohio 43210*

Synopsis

To facilitate the study of new reaction injection molding (RIM) materials on a practical scale, a lab-scale mini-RIM machine was constructed. This machine is capable of delivering up to approximately 250 cc of material at rates of up to 125 cc/s. The RIM machine was first tested with conventional materials such as crosslinked and linear polyurethanes. The effect of varying the nozzle Reynolds number upon the adiabatic temperature rise corresponded to the results reported in previous works. Following this verification, two developmental materials, a polyurethane/polyester interpenetrating polymer network and a polyurea, were examined. The polyurea material showed a very strong dependency on mixing up to a Reynolds number above 400. The 75/25 PU/PEster reaction exotherms also showed a dependency upon mixing. However, this dependency is noticeable only in the polyester portion of the reaction, which can be attributed to the mixing sensitivity of the redox-type initiators used.

INTRODUCTION

The major commercial reaction injection molding (RIM) materials used today are polyurethanes. The reason is that polyurethane systems are able to provide fast, complete reactions with a wide range of physical properties through the incorporation of cross-linking, domain-forming, fiber-reinforcing, and foaming additives. Other materials which can be processed by RIM include nylon, epoxy, polyester, and silicon rubber.^{1,2} However, none of them have yet met with wide-scale commercial acceptance.

To increase the reaction rate and provide better physical properties, many RIM products, especially in automotive applications, have shifted from using polyurethane to polyurethane/urea.³ The difference in these systems is that the chain extender used is a low-molecular weight diamine in place of the short chain diol. The diamines are much more reactive than the diols and build resin viscosity much faster, thus creating less turbulence during mold filling and resulting in faster and cleaner demolding. Today, diethyl toluene diamine (DETDA) is the major chain extender used in this type of system.

Since the urea linkage is more thermally stable than the urethane linkage, many researchers have been working on producing a total polyurea resin for RIM applications. In these systems, amine chain extenders are used and the long-chain polyols of the polyurethane system would also be replaced by amine-terminated polyether resins.⁴⁻⁸ The major difficulty in processing this material is its extremely fast reaction speed. Even uncatalyzed, this system

*To whom correspondence should be addressed.

reacts much faster than conventional urethane systems, with less than one second gel times being typical. These high reaction rates are too fast to allow filling of complex commercial molds using the current RIM machinery.⁴ Initial studies of the kinetics of this system have shown that the chain extension reaction occurs almost instantaneously upon mixing,^{4,5} leading to the rapid viscosity rise and the subsequent mold-filling difficulties. Many researchers are presently working to develop slower reacting chain extenders by modifying the chemical structure of the diamines (e.g., using steric hindrance from side groups to reduce the amine's reactivity).^{6,7}

Another method for improving the properties of RIM materials is internal reinforcement of the polyurethane polymer matrix with another polymer. In RIM, the monomers for the two resins are mixed and allowed to react simultaneously within the mold to produce a highly entangled mixture of the two resins. This approach is commonly referred to as simultaneous interpenetrating polymer networking (IPN) of the two resins. The advantage of using an internal reinforcement over traditional external reinforcing is that a low-viscosity resin is added to the system instead of a highly viscous inert filler; thereby avoiding the problems of machine wear and property variation with flow direction commonly associated with the fiber-filled resins.

Most IPNs commercially available have been developed for slow processes such as casting and coating. For RIM applications, there are only a few commercially available IPN compounds. Ashland Chemical Company has developed a RIM system based on an unsaturated polyol chain which is networked with a crosslinking agent, acrylic monomer.⁸ Amoco Chemical Company has developed a series of polyester-urethane hybrids which can be used in the RIM process.⁹ Similar polyurethane-polyester IPNs have also been studied by Nguyen and Suh^{10,11} and Hsu and Lee.¹² These systems are based on a linear polyurethane matrix being reinforced by a crosslinked polyester resin. The previously mentioned investigations have shown that the mechanical and morphological properties of these systems are highly dependent upon the processing conditions used. This dependency is attributed to the competitive nature of the two reactions and the effect the processing conditions have on the balance between the two.

In this study, the mixing characteristics of several RIM materials, including a crosslinked polyurethane, a segmented linear polyurethane, a polyurethane/polyester IPN, and a polyurea resin, were evaluated. Experiments were carried out using a laboratory scale RIM machine. The degree of mixing was determined by measuring the adiabatic temperature rise, visual examination, and thermal analysis of the molded samples.

APPARATUS

Lab Scale RIM Machine

Due to the large size and cost of commercial RIM machines and the high volumes of material necessary to flush and operate them, several researchers have developed lab-scale RIM machines for conducting feasibility studies involving RIM materials. These machines use smaller, less expensive drive systems such as a lever-arm with one drive cylinder,¹³ or conventional hydraulic drive systems.¹⁰ For the lever-arm machine, the ratio of the reactants

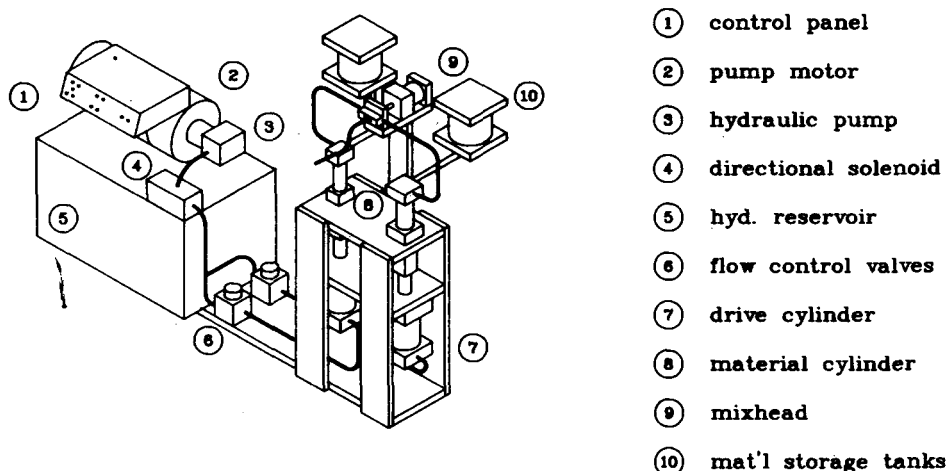


Fig. 1. Schematic diagram of the lab-scale RIM machine.

is controlled by the location of the pivot point of the lever arm. This is an elegant way to control the ratio of the two streams, but is geometrically restrictive of the material ratios which can be run. The geometric restrictions come from the radial components of force imparted to the pistons by the lever arm and by physical limitations as to how short the lever arm could be made.

Nguyen and Suh designed a RIM machine¹⁰ which has overcome this ratio limitation by using individual drivers for each of the material cylinders. Thus, almost any ratio of materials can be produced. The disadvantage of this type of system is that since the ratio is not mechanically fixed, it must be measured for each shot and varies with the accuracy of the control scheme. The machine is also more expensive than the lever-arm type.

In this study, a lab-scale RIM machine similar to but simpler than that made by Nguyen and Suh¹⁰ was constructed. This machine is shown in Figures 1 and 2, which is capable of delivering up to ca. 250 cc of material at rates up to 124 cc/s (actual deliveries depend strongly upon material ratios). Using a 1/4-inch diam mixhead with 1/32-inch diameter nozzles, these flow rates are able to produce maximum nozzle Reynolds numbers in the order of 300 to 500 with the RIM systems explored in this work. This range of Reynolds number is similar to that obtainable on commercial machinery. The machine's reasonably small size, roughly 2 ft (61 cm) wide by 5 ft (152 cm) long by 5 ft (152 cm) high, and weight, roughly 600 lbs (273 kg), allows it to be easily rolled from room to room, which allows for flexibility in interfacing the RIM machine with other analytical devices.

The basic components of the RIM machine are shown schematically in Figure 1. Both the hydraulic drive system (items 1-7) and the material mixing system (items 8-10) are attached to a common support frame. The hydraulic drive unit consists of 7.5 hp variable flow hydraulic pump and its 10 gallon hydraulic oil reservoir. An adjustable maximum pressure-controlling circuit bleeds the high pressure pump output back to tank as necessary to maintain a consistent output pressure. A three-position directional solenoid valve is used to control the direction of drive piston's travel and to prevent cylinders from moving when the solenoid is not activated. Flow rates into the individual



Fig. 2. Photograph of the lab-scale RIM machine.

drive cylinder are controlled by unidirectional flow control valves (Double A model QXA-005-10A1).

The drive cylinders for this RIM machine are 3.25 in. (8.26 cm) diam hydraulic cylinder with a stroke of 3 in. (7.62 cm) (Mosier Model H3.25CX3). These cylinders are connected directly to the material cylinders containing the reactants. The three material cylinders available for use on this machine are 3-in. (7.62 cm) stroke water service hydraulic cylinders with Vitron seals and have the following diameters: 1.5 in. (3.81 cm), 2 in. (5.08 cm), and 2 in. (5.08 cm) (Mosier Models H1.5CX3, H2CX3, and H2CX3-SS). All material cylinders have chrome-plated inner surfaces, carbon steel end caps, and brass pistons with the exception of the one 2 in. (5.08 cm) cylinder with the SS designation, which has entirely stainless steel construction. This stainless steel construction was chosen for use with peroxide-containing reactants to prevent catalyzation with iron oxides or other metals. The smaller diameter material cylinders provide 2.6–4.7 times increase in the system pressure from the driver system to the material system.

Reactants are loaded into the material cylinders via the filling ball valves. These valves are generously sized so as to permit easy filling of viscous materials. Filling is aided by pressurizing the material tanks with nitrogen gas, which also serves to prevent atmospheric moisture from contaminating the reactants. Because of the vertical set-up, any air which may be trapped in the system can be removed by bleed valves located adjacent to the pressure transducers and at the highest point in the material system.

The mixhead and its driving cylinder was described by Lee and Macosko.¹³ When the mixhead plunger is in its forward position, it blocks both nozzles to prevent material leakage. As the mixhead driver cylinder is activated, the plunger is pulled back to permit mixing within the chamber.

To make a shot, the solenoids controlling the drive cylinders and the mixhead drive cylinder are activated simultaneously. Since the filling ball valves are closed, all of the material is forced through the mixhead and then to the mold. Once the required amount of reactants are mixed, the solenoids are deactivated, the mixhead closes, and the drive cylinders stop. The progression of the reaction within the mold can be followed by thermocouples and viscometers within the test mold, which record the temperature rise as well as the viscosity rise of the material.

Following the shot, the filling valves are opened to relieve any residual pressure and to let material refill the cylinder as the pistons are lowered. Temperature control for the reactants was obtained by enclosing the entire material system within a temperature-controlled chamber. The air in the chamber was heated by a heat gun and was then circulated using several small blowers to provide uniform heating of the materials. This system maintained the materials within approximately 1°C of the set point (30 to 80°C). Additionally, the heating chamber serves as safety shield for containing leaks and vapors from the reactants.

To confirm the proper operation of the RIM machine and to follow the reaction of molded material, the electrical signals from several transducers were recorded. An IBM XT personal computer was used to digitally record the temperature and viscosity measurements as well as several other machine transducers, including material line pressure transducers and cylinder displacement LVDTs. All of these transducers were connected to the PC using a Metrabyte STA08 connection board attached to the internal A/D converter

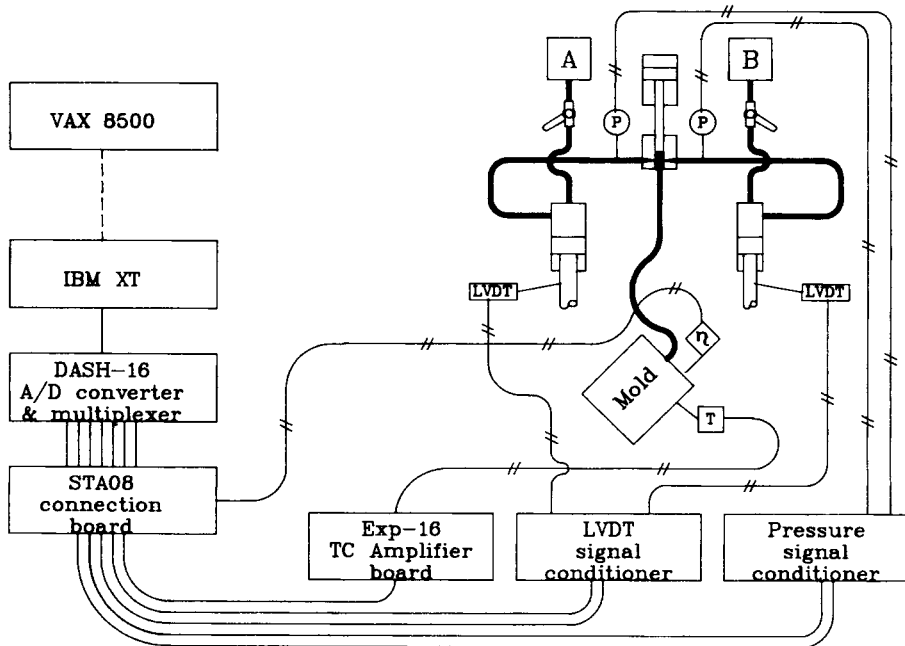


Fig. 3. Data acquisition schematic diagram.

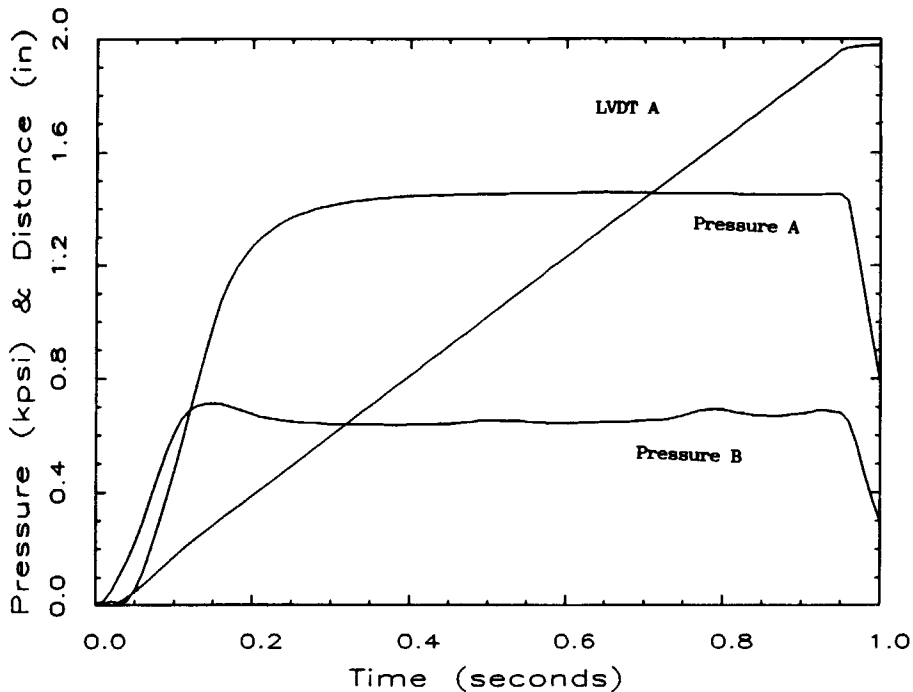


Fig. 4. Typical LVDT and pressure traces during injection. Material used is polyurea resin.

of the computer, a Metrabyte Dash-16 converter and multiplexer. This system is shown schematically in Figure 3.

Machine Calibration

The stability of the pumping system was evaluated. The length of travel during a 1-s shot of each of the material cylinders was measured using a caliper and its travel was followed using the LVDTs. The LVDT traces were used to show that the variation in the cylinder travel speed was negligible and that the average velocity determined by means of the caliper measurements were representative of the actual travel velocities of the cylinders. A sample LVDT trace during a polyurea run is shown in Figure 4. The results of the caliper measurement during this testing showed the repeatability of the shot travel distance to be within the measurement accuracy ($\pm 0.3\%$) which resulted in a velocity ratio accuracy of $\pm 1\%$.

Also shown in Figure 4 are typical traces of the mixing pressures for the reactants of polyurea. These traces show the transitional flow region during approximately the first 0.2 s of the shot in which the pressure increases from zero to the steady-state shot pressure. The LVDT trace shows that although the system pressure may be changing during this transition period, the cylinder speed is only slightly affected by the change.

To further evaluate the stability of the mixing in the RIM machine throughout the shot, a long Tygon tube was attached to the mixhead, which was spiralled upward around a flask to prevent air entrapment as the tube was filled. This molding allowed comparison of the molded material at differing portions of the shot since little back mixing occurred in the tube. The

molded samples showed consistent color and complete reaction throughout the tube, which indicated that the material ratios were consistent through the shot. The samples also showed that the majority of the shot was free of air bubbles, with only first 10% of the material having a significant number of bubbles trapped. This material is near the flow front and appears to have trapped the air as the material filled the mixing chamber and then filled the empty tube.

In order to set the desired flow rate on each stream, it is necessary to establish a flow rate calibration curve for the flow control valves. It was found that setting of the second valve affected the flow rate through the first valve slightly, however, the calibration curve so established still provided a reasonable first guess for the valve setting and greatly reduced the shot setup time. Once the valves were set, a test shot could be made back to the material tanks by leaving the filling ball valves open and disconnecting the mixhead solenoid. Following the test shot, the distance each cylinder traveled could be measured and the valves adjusted to provide the correct speed. Since no material was used, this procedure could be repeated as many times as necessary to obtain the correct flow rate. For typical shots, the initial valve setting could provide velocities within 10% of the desired values. With one adjustment, the velocities were within 1%.

EXPERIMENTAL

Materials

Crosslinked Polyurethane (CPU)

The crosslinked polyurethane system evaluated was formed by reacting a liquid form of 4,4'-diphenylmethane-diisocyanate, MDI (Dow, 143-L), with a polyester triol with an average molecular weight of 533 (Union Carbide, TONE 305). 0.1% by weight of dibutyltin dilaurate catalyst (M & T Chemical, T-12) was added to produce a material with a gel time of 7 seconds at an initial material temperature of 51°C. A 5% molar excess of MDI was used to ensure complete reaction. This formulation is summarized in Table I.

Segmented Linear Polyurethane (LPU)

The linear polyurethane system evaluated in this work was prepared by reacting MDI (Dow, 143-L) with a long chain diol (2000 MW) based on poly(ϵ -caprolactone diol) (Union Carbide, T0240) to produce the soft segment and a short-chain diol chain extender (90 MW), 1,4-butanediol (Aldrich Chemical, BDO), to produce the hard segment. The molar ratio of the materials used was approximately 6/1/5 143-L/T0240/BDO. A 5% excess of MDI was used to ensure complete reaction. This resulted in the formation of an elastomeric polyurethane with a solidification time of 2 s at an initial material temperature of 55°C and 0.6% by weight of T-12 catalyst. This formulation is also summarized in Table I.

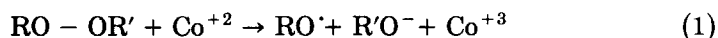
Polyurethane / Polyester Interpenetrating Polymer Network (IPN)

The IPN system examined in this work was based on the linear polyurethane system described before combined with an unsaturated polyester

TABLE I
Formulations of Urethane-Based RIM Materials Used in This Work

	Parts by volume		
	CPU	LPU	IPN
Polyurethane			
MDI (Dow 143-L)	40.6	36.2	28.2
Diol (UC T0240)	—	50.4	36.9
Diol (Aldrich BDO)	—	13.4	9.9
Triol (UC T0305)	59.4	—	—
T-12 (Air Product)	0.1 wt	0.6 wt	0.6 wt
Polyester			
Unsaturated Polyester (Ashland Q6585)	—	—	15.8
Styrene	—	—	9.2
PDO (Lucidol)	—	—	6.9 wt
Co-8 (Fluka Co.)	—	—	4.0 wt
Resin gel time (s)	7	2	15

resin (Ashland Q6585) and its crosslinking agent, styrene monomer. One volumetric ratio, 75/25, of polyurethane to polyester was examined in this study. The catalyst and initiator levels were set at 0.6% by weight of T-12 in the polyurethane phase and 6.9% by weight of PDO (Lucidol) with 4.0% by weight of cobalt naphthenate promoter (Fluka Co., Co-8) in the polyester phase. The addition of cobalt to the reaction changes the PDO decomposition reaction from a thermally initiated reaction to a reduction oxidation-type reaction:



This initiator/catalyst combination resulted in a gel time of the system around 15 s at an initial temperature of 55°C. This formulation is also summarized in Table I. The polyester resin and the cobalt promoter was added to the isocyanate side of the formulation while the PDO initiator was added to the polyol side with the urethane catalyst, T-12.

Polyurea

The ingredients of the polyurea used in this study are summarized in Table II. The recipe consists of a soft segment based on a high-molecular weight (5000 MW) triamine (Texaco Chemicals, Jeffamine T5000) and a hard segment based on MDI (Dow 1305) chain extended with a short-chain (89 MW) diamine, tert-butyl toluene diamine (TBTDA) (Air Product). The 1305 MDI is a blend of isocyanate (50% by weight) and a high-molecular weight polymer

TABLE II
Formulation for Polyurea RIM Material Used in this Study

Ingredient	Weight percentage
Diisocyanate (DOW 1305)	43.5
Diamine (Air Product TBTDA)	17.0
Triamine (Texaco T5000)	39.5

(50% by weight) with an equivalent weight of 210. The molar ratio used was T5000/1305/TBTDA = 11.1/100.0/88.9 (70/77/30 by weight), which is typical of commercial RIM formulations. This formulation produced a crosslinked polyurea with a gel time of < 1 s. This fast reaction precluded the use of the Brookfield viscometer for viscosity measurements and made temperature measurements difficult since the material solidified before it would flow around the thermocouple. To facilitate thermal measurements, the thermocouple was placed directly across from the mixhead opening to assure the thermocouple would be surrounded by material before the resin could solidify.

All materials were used as received with the following procedures taken to reduce molding difficulties. To prevent foaming all of the materials processed has to be degassed prior to use. This was especially important for the polyols and amines since they absorbed atmospheric moisture. These materials were degassed under vacuum overnight at 50°C. The isocyanate was degassed at room temperature for about 2 h. Both materials were preheated to about 55°C on a hot plate to shorten the heat-up time in the RIM machine. It was also necessary to use nitrogen gas to purge the air space in the isocyanate storage tank to prevent reaction with the moisture in the ambient air.

Experimental Setup

For each of these resin systems, the pretreated materials were loaded into the material tanks inside of the temperature control chamber of the lab-scale RIM machine. The materials were gently stirred in these tanks for 1 h to obtain thermal equilibrium. The material was then filled into material cylinders of the machine. During the shot, the material was mixed and fed to an insulated paper cup by means of Tygon tubing. A thermocouple and a viscometer probe located in the cup provided information on the adiabatic temperature rise and the viscosity rise of the resin during its reaction.

Following verification of material flow rate by caliper measurement, the flow control valve settings were then changed to permit examination of the next flow rate condition. This procedure was repeated until all of the material in the storage tanks was used. If the material volume permitted, repeat runs at several velocities were attempted. The cup samples were cut in half using a bandsaw to permit cross-sectional viewing for comparative mixing measurements. To understand the effect of mixing on the crystallinity structure of samples containing linear polyurethane, these samples were tested by differential scanning calorimetry (Perkin-Elmer DSC-2C) in the scanning mode by heating from room temperature to 200°C with a heating rate of 10°C/min.

RESULTS AND DISCUSSION

Polyurethanes

Figure 5 shows the adiabatic temperature rise curves for the crosslinked polyurethane system after impingement mixing at different nozzle Reynolds numbers, where Reynolds number is defined as follows:

$$N_{Re} = \frac{4Q\rho}{\pi D\eta} \quad (2)$$

Reynolds Number Effect on Crosslinked Polyurethane Reaction

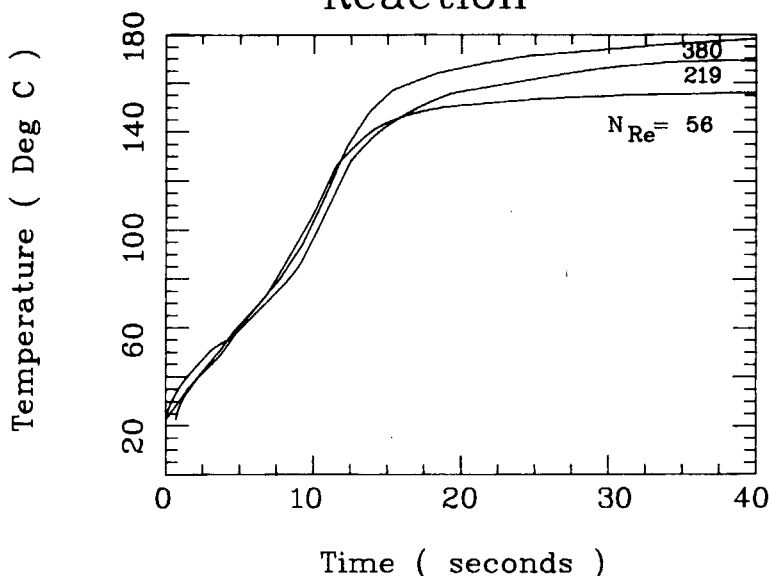


Fig. 5. Effect of nozzle Reynolds number on adiabatic temperature rise of CPU RIM. $t_{gel} = 7$ s. $T_0 = 51^\circ\text{C}$.

where Q is volumetric flow rate, ρ is density, D is nozzle diameter, and η is the viscosity of the more viscous stream. From this figure, it can be seen that although the initial reaction rate (up to approximately 15 s) does not show too much dependency upon Reynolds number, the ultimate temperature rise does. The figure shows that the ultimate temperature rise, and consequently the ultimate conversion, decreases as the N_{Re} decreases. This is to say, that material properties that depend upon the initial reaction rate, such as gel time, do not show a strong dependency on N_{Re} , while material properties which depend on final conversion, such as mechanical properties, do show a dependency at lower Reynolds numbers.

Figure 6 shows similar curves for the linear polyurethane system. The LPU system, however, does not show the strong dependency on mixing that the crosslinked system does. In fact, within the experimental variation, there is no noticeable dependency of the ultimate temperature rise of the LPU system upon Reynolds number.

Cross sections of the molded polyurethanes were also examined. For the linear PU system, no visible difference is noticeable as the Reynolds number was varied, with the exception of increased air entrapment in the sample molded at the highest Reynolds number. The bulk of the material is homogeneous and no area of poor mixing are evident. For the crosslinked PU system, however, the lowest N_{Re} sample shows signs of unreacted monomer and poor mixing while the samples with N_{Re} greater than 200 appear much more uniform and completely reacted. These results are in general agreement with

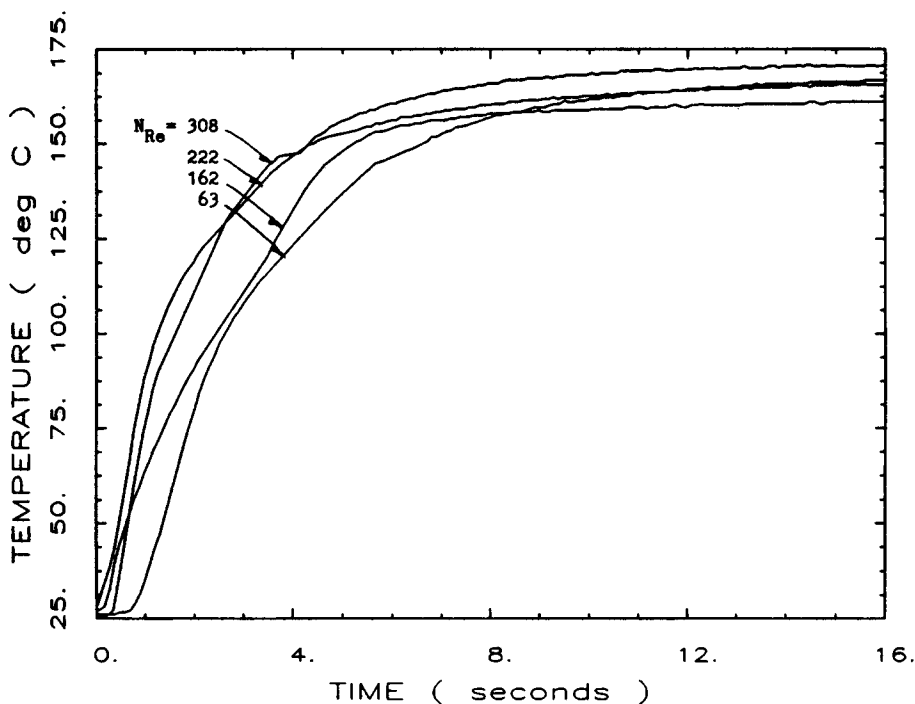


Fig. 6. Effect of nozzle Reynolds number on adiabatic temperature rise of LPU RIM. solidification time = 2 s. $T_0 = 55^\circ\text{C}$.

the findings of previous works. Lee et al.¹⁴ showed a critical Reynolds number of about 200 for a similar crosslinked PU system, while Kolodziej et al.¹⁵ showed that linear PUs were less mixing dependent than the crosslinked systems.

PU / P Ester IPNs

The results of the adiabatic temperature rise for this system are shown in Figure 7. It is quite apparent that the reaction system is highly dependent on the Reynolds number, with the reaction rate decreasing with decrease in the Reynolds number. It is also apparent that the reaction exotherm has two distinct stages, or humps. The first hump can be attributed to the polyurethane reaction while the second overlaying hump is attributed mainly to the polyester reaction.¹² The polyurethane reaction does not show a dependency on N_{Re} , which has been previously shown to be the case for the linear polyurethane used. The polyester reaction, however, shows a strong dependency upon N_{Re} both in induction time (the time before the second peak starts) and the ultimate height of the exotherm. These dependencies can be explained by the initiator used. The initiator, Co-8 and PDO, gives a redox-type reaction system, and would be expected to exhibit a mixing dependency since the two components must come into contact in order to react. The induction time of the free radical polyester is indicative of the free radical concentration within the mixture since the inhibitor level is constant for all the samples. Thus, the longer induction times for the lower Reynolds number cases indi-

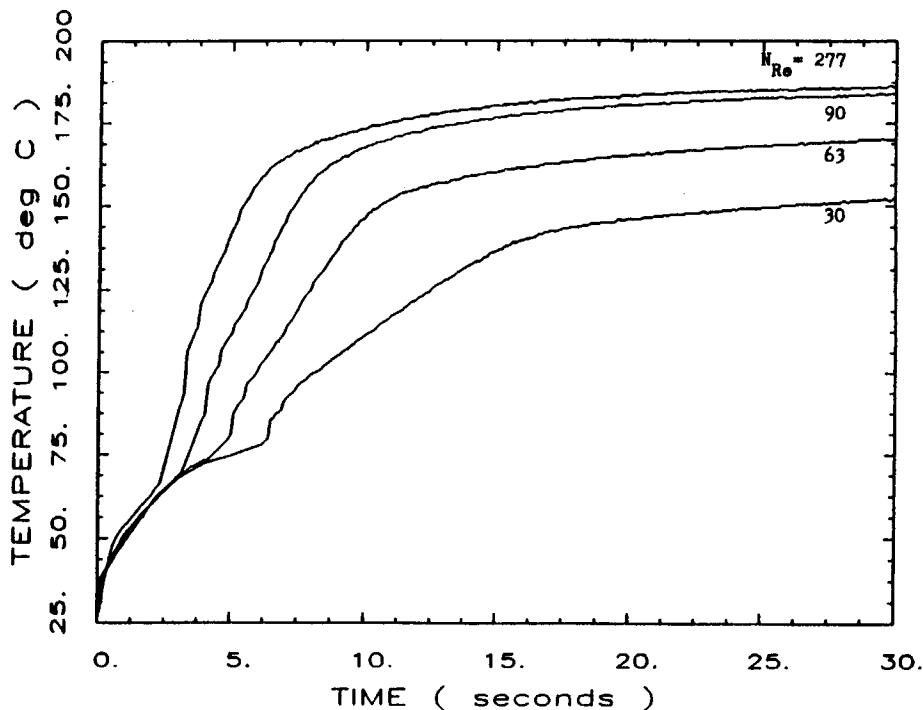


Fig. 7. Effect of nozzle Reynolds number on adiabatic temperature rise of IPN RIM. $t_{gel} = 15$ s. $T_o = 55^\circ\text{C}$.

cate that less free radical is being generated. Examination of the cross sections of the molded samples also shows a dependency on the Reynolds number, which is in general agreement with the temperature rise data.

Polyurea

Another RIM resin system examined in this study was polyurea. Figure 8 shows the effect of varying the Reynolds number on the adiabatic temperature rise for this system. It can be easily seen that the dependency on N_{Re} is very great even up to the N_{Re} as high as 400. The overall reaction rate as well as the ultimate temperature rise of the system decreases as the Reynolds number decreases. The effect of Reynolds number on the maximum adiabatic temperature rise is shown in Figure 9. In this figure, it is apparent that for N_{Re} less than the critical N_{Re} of approximately 375 there is a strong dependency of the temperature rise upon the Reynolds number. For N_{Re} greater than 375, although the dependency appears to be much lower, there does appear to be some dependency of the reaction rate upon Reynolds number as shown in Figure 8.

The cross section of several samples of the polyurea material was examined visually. The poor mixing of the lower Reynolds number samples is very apparent by the unreacted monomer shown at the surface of these samples. The small monomer droplets and slight color streaking through the sample indicate that this material was not completely mixed even at the highest Reynolds number. Therefore, for a complete reaction in this polyurea system, a Reynolds number greater than 438 will be necessary.

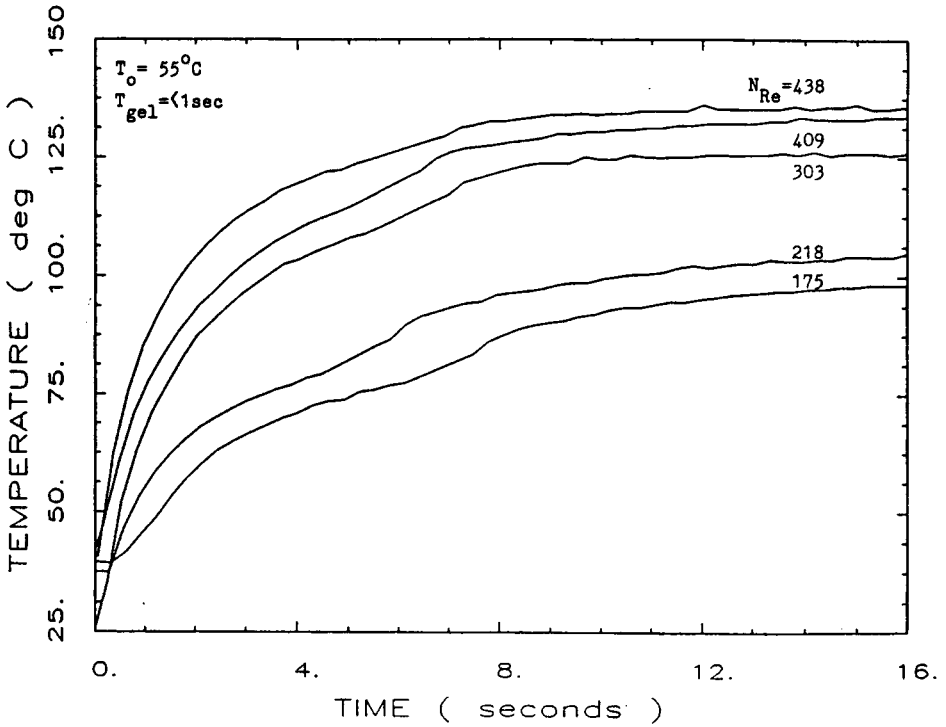


Fig. 8. Effect of nozzle Reynolds number on adiabatic temperature rise of polyurea RIM. $t_{gel} < 1 \text{ s}$. $T_o = 55^\circ$.

Reynolds Number Effect on Temperature Rise of Various RIM Materials

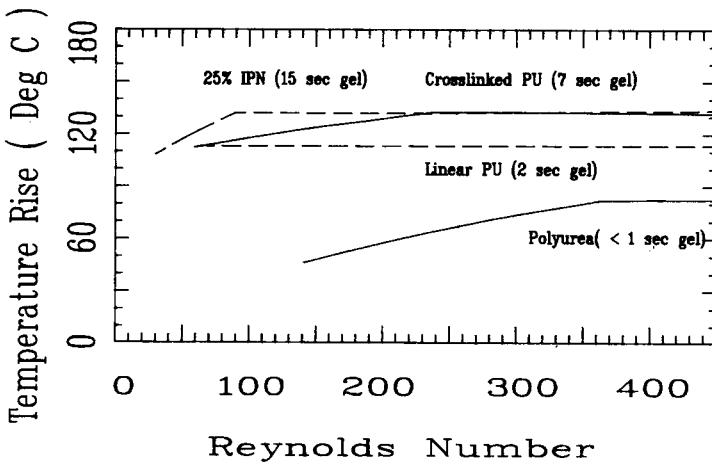


Fig. 9. Maximum adiabatic temperature rise vs. nozzle Reynolds number for four RIM materials.

SCANNING DSC RESULTS

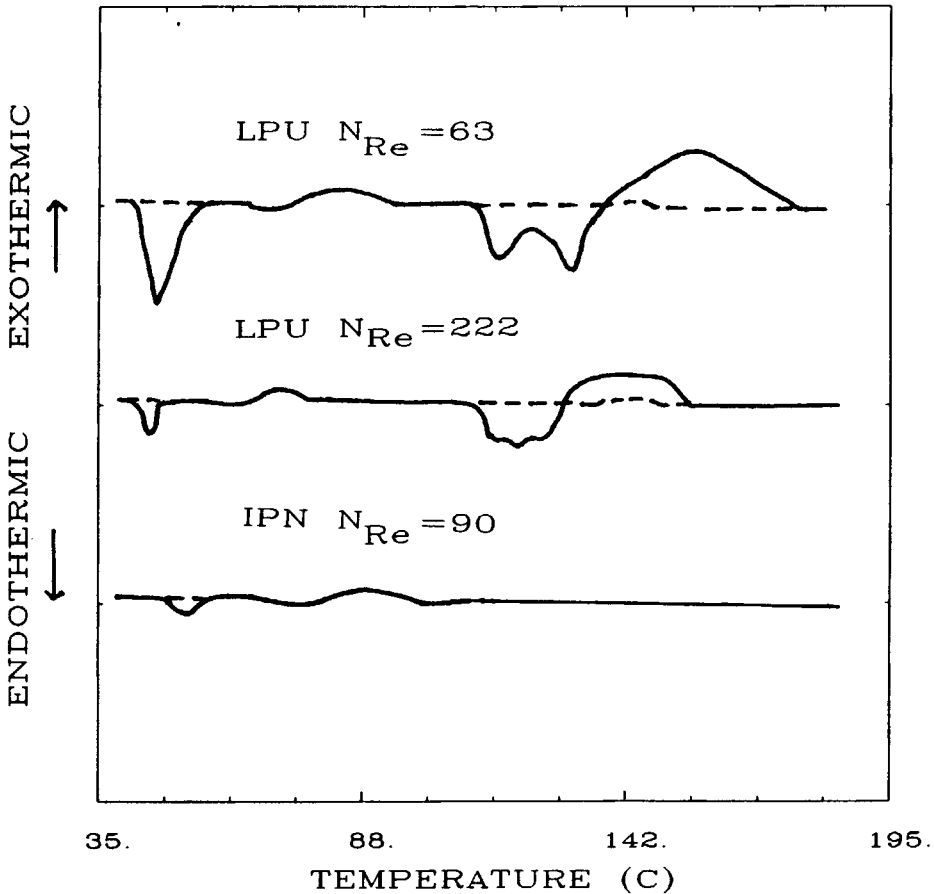


Fig. 10. Scanning DSC results for samples containing linear PU.

Figure 9 also offers a comparison of the Reynolds number dependency for each of the systems discussed herein. Several key features should be noted from this summary. The first feature is the lower exotherm produced by the polyurea reaction. This lower exotherm would generate lower thermal stresses within the molded part and may produce better products. The drawback to the polyurea system can be seen from the high Reynolds number necessary to obtain adequate mixing for the system. It can also be noted that in general, as the reaction rate of the system increases (its gel time decreases), its dependency on mixing increases (its critical Reynolds number increases). The exception to this observation is the linear PU system shown in the figure. An explanation for this difference lies in the difference in the mechanism of solidification for the linear and crosslinked PU systems. The solidification effect in the linear PU system has been attributed to phase separation¹⁶ as opposed to chemical crosslinking in the other system. It seems that phase separation may not produce the barriers to molecular diffusion as chemical crosslinking does. Thermal analysis by DSC shown in Figure 10, however, indicates that the crystal structure in RIM molded LPU is mixing dependent.

At low Reynolds numbers (e.g., $N_{Re} = 63$) a large soft domain melting peak at 40–55°C, and two hard domain melting peaks at 115–137°C are observed, followed by an exothermic peak (1.4 cal/g). As the degree of mixing was increased from $N_{Re} = 63$ to 222, the soft domain melting peak becomes much smaller and the hard domain melting peaks also become smaller and tend to merge together, followed by a small exothermic peak (0.5 cal/g). Several researchers^{15,17} have pointed out that, for a diffusion-controlled urethane polymerization, the formation of soft and hard domains depends strongly on the extent of mixing. Poor mixing causes reactant segregation, and reaction has to rely on the interdiffusion of the monomer species. For LPU, the small, more mobile chain extender molecules can diffuse into the isocyanate side to form large hard blocks, while the relatively immobile long chain diols can only react with diisocyanate molecules which diffuse in from the isocyanate side. Such a diffusion-caused separation effect may result in a higher extent of phase separation and, consequently, larger melting peaks of hard and soft domains observed in thermal analysis. Good mixing tends to increase random copolymerization and reduce the block size of hard and soft segments, which in turn, decreases the melting peaks observed in thermal analysis. The exothermic peaks in Figure 10 indicate the existence of small residual reactivity (10% for $N_{Re} = 63$, 3% for $N_{Re} = 222$) and possibly recrystallization. These results suggest that for linear polyurethanes, the measurement of adiabatic temperature rise is not an appropriate method for mixing characterization. Figure 10 also shows the scanning DSC result for an IPN sample with $N_{Re} = 80$. Except a small soft domain melting peak, there is no hard domain melting peaks. This is also true for other IPN samples. Apparently, the existence of polyester resin prevents the formation of hard domain crystal.

CONCLUSIONS

The lab-scale RIM machine constructed is suitable for processing RIM materials and preparing samples for evaluation. This machine can process materials with up to 4 to 1 volumetric ratios and can maintain the overall shot ratio of the materials to within 1% of the desired value.

The effect of nozzle Reynolds number on the reaction of a 75/25 polyurethane/polyester IPN resin showed that a critical Reynolds number of 90 was necessary to obtain good mixing. This effect was shown to be attributed to the polyester reaction as a result of the redox initiator used. The effect of the nozzle Reynolds number on the reaction of a polyurea system with less than 1 s gel time was shown to be greater than the other resin systems studied. In this resin, the critical Reynolds number for good mixing was higher than 400. For Reynolds numbers less than 400, the reaction rate dropped off greatly and a large amount of unreacted resin was noted in the samples. Even for Reynolds number greater than 400, the resin appears to still exhibit some dependency upon mixing.

The authors would like to thank the Engineering Research Center of Net Shape Manufacturing at OSU and General Motors Corporation for financial support. Material donation from Union Carbide Corporation, Texaco Chemical Company, and Ashland Chemical Company is greatly appreciated. The authors would also like to thank Mr. G. Ferber of GM and Mrs. T. J. Hsu and R. A. Kelch for their help and valuable discussions.

References

1. L. J. Lee, *Rubber Chem. Tech.*, **53**, 542 (1980).
2. C. W. Macosko, *Plast. Eng.*, 21 (April 1983).
3. E. C. Steinle, F. E. Critchfield, J. M. Castro, and C. W. Macosko, *J. Appl. Polym. Sci.*, **25**, 2327 (1980).
4. N. P. Vespoli and L. M. Alberino, *Polym. Proc. Eng.*, **3**, 127 (1985).
5. M. C. Pannone, M.S. Thesis, University of Minnesota (1986).
6. A. S. Wood, *Mod. Plast.*, 48 (October 1984).
7. J. A. Sneller, *Mod. Plast.*, 55 (February 1986).
8. W. L. Kelly, *Plast. Eng.*, 29 (February 1986).
9. H. R. Edwards, *SPE ANTEC Papers*, 1326 (1986).
10. L. T. Nguyen and N. P. Suh, *Polym. Proc. Eng.*, **3**, 37 (1985).
11. L. T. Nguyen and N. P. Suh, *Polym. Proc. Eng.*, **26**, 843 (1986).
12. T. J. Hsu and L. J. Lee, *Polym. Eng. Sci.*, **25**, 951 (1985).
13. L. J. Lee and C. W. Macosko, *SPE ANTEC Papers*, **24**, 151 (1978).
14. L. J. Lee, J. M. Ottino, W. E. Ranz, and C. W. Macosko, *Polym. Eng. Sci.*, **3**, 57 (1980).
15. P. Kolodziej, C. W. Macosko, and W. E. Ranz, *Polym. Eng. Sci.*, **22**, 288 (1982).
16. R. E. Camargo, C. W. Macosko, M. Tirrell, and S. T. Wellinghoff, *Polym. Eng. Sci.*, **22**, 719 (1982).
17. S. O. Fields and J. M. Ottino, *AIChE J.*, **33**, 959 (1987).

Received September 28, 1987

Accepted January 19, 1988